

Magnetocaloric effect and its implementation in critical behaviour study of $\text{La}_{0.67}\text{Ca}_{0.33}\text{Mn}_{0.9}\text{Fe}_{0.1}\text{O}_3$

R M'NASSRI^{1,2} 

¹Higher Institute of Applied Sciences and Technology of Kasserine, Kairouan University, BP 471, 1200 Kasserine, Tunisia

²Laboratoire de Physico-Chimie des Matériaux, Département de Physique, Faculté des Sciences de Monastir, Université de Monastir, 5019 Monastir, Tunisia

MS received 4 August 2015; accepted 8 February 2016

Abstract. The magnetocaloric effect (MCE) and the field dependence of the magnetic entropy changes in the perovskite-type $\text{La}_{0.67}\text{Ca}_{0.33}\text{Mn}_{0.9}\text{Fe}_{0.1}\text{O}_3$ were studied using the phenomenological model. The model parameters were determined from the magnetization data adjustment and used to give better fits to magnetic transition and to calculate the magnetocaloric properties. The entropy curves have been observed to behave a symmetrical broadening of ΔS_M peak with the increase in magnetic field. The values of maximum magnetic entropy change, full-width at half-maximum, relative cooling power (RCP) and the refrigerant capacity (RC), at several magnetic field variations, were calculated. The maximum magnetic entropy change of $1.17 \text{ J kg}^{-1} \text{ K}^{-1}$ was obtained for 3 T. The theoretical calculations were compared with the available experimental data. The results were found to be in good accordance. The critical exponents associated with ferromagnetic transition have been determined from the MCE methods. By using the field dependence of $\Delta S_{\text{max}} \approx a (\mu_0 H)^n$ and the RCP $\approx v (\mu_0 H)^w$, the critical behaviour of $\text{La}_{0.67}\text{Ca}_{0.33}\text{Mn}_{0.9}\text{Fe}_{0.1}\text{O}_3$ was investigated. From the analysis of the relationship between the local exponent n and w , other exponents β , γ and δ were calculated. Our results indicated that the ferromagnetic coupling in the $\text{La}_{0.67}\text{Ca}_{0.33}\text{Mn}_{0.9}\text{Fe}_{0.1}\text{O}_3$ can be well described by the 3D Heisenberg model. This reflects an existence of ferromagnetic short-range order in the sample.

Keywords. Model; manganites; magnetization; magnetocaloric effect; critical exponent.

1. Introduction

Large number of magnetocaloric effect (MCE) materials have attracted much attention owing to their numerous potential advantages over vapour-compression refrigeration: higher chemical stability, easy fabrication, longer usage time, low noise, etc. [1–5]. For an overview on the experimental and the theoretical aspects of the (MCE), see references [6,7]. A lot of work has been carried out by various researchers with the aim to understand physics of perovskite-manganites and to explore possible applications such as MCE [8–12]. These materials exhibit a large magnetization change under the application of a magnetic field. They transform from a magnetically disordered state to an ordered state (at a temperature close to its critical temperature), and consequently large magnetic entropy changes occur [1]. Several compounds with a high MCE can be elaborated at different (low, intermediate and high) temperatures, and the major problem remains to get the samples with a high MCE at a low external magnetic field, which is advantageous for application as magnetic cooling, working in the fields produced by permanent magnets [13]. Manganites are promising candidate materials to satisfy this requirement and might be of the option of future magnetic cooling [14–16]. These perovskites

are characterized by the strong competition among a ferromagnetic double-exchange (DE) interaction, an antiferromagnetic super-exchange interaction and the spin–phonon coupling [17–19]. Magnetic and magnetocaloric properties of these interactions are determined by intrinsic parameters such as, doping level [20], average cationic size [21], cationic disorder [22], grain boundary [23], sintering temperature [24], particle size [25] and oxygen stoichiometry [26].

Phan *et al* [27] studied in their review the MCE in manganites systems and they have explained that the large MCE in the perovskite manganites can originate from the spin–lattice coupling related to the magnetic ordering process. This strong coupling is evidenced by the lattice changes accompanying the magnetic transitions in these manganites; the lattice structural change in Mn–O–Mn bond angles and Mn–O bond distances with temperature, which results in a variation of the volume, can cause an additional change in the magnetic properties of the material. There is no doubt that manganese ions play a crucial role in the DE process. Hence, it is worthwhile to investigate the influences of the replacement of Mn by other transition metals. Several works have been made on the effects of the substitution at Mn site by various elements. They suggested that the introduction of a transition element Cr [28,29], Co [30,31] and Fe [32,33] commonly affected the magnetic and electrical properties in manganites systems. It is found that when modifying the

(rafik_mnassri@yahoo.fr)

Mn element in ferromagnetic manganites always leads to a reduction in T_C and magnetization, an increase in the resistivity and ultimately insulating state at low temperatures for high substitutions.

To obtain a large ΔS_M material without a thermal and magnetic hysteresis which is workable in a wide range of temperatures, Mukadam *et al* have studied the effect of the doping of Fe in $\text{La}_{0.67}\text{Ca}_{0.33}\text{MnO}_3$ manganites [34]. Iron was chosen as the dopant because Mn^{3+} and Fe^{3+} have ionic radii that are close to each other and hence the crystal structure of the material remains almost unaltered [34]. Since the spin, charge, lattice and orbital degrees of freedom are intimately linked to the Mn ion, any perturbation at the Mn site is expected to modify ground state properties of such manganites. In a mixed system of Fe and Mn, the Fe^{3+} ions do not participate in the DE interaction with Mn^{3+} ions. Thus, the ferromagnetic DE interaction is weakened to the profit of superexchange interactions which favours the antiferromagnetic coupling between $\text{Mn}^{4+}\text{-O-Mn}^{4+}$, $\text{Mn}^{4+}\text{-O-Fe}^{3+}$ and $\text{Fe}^{3+}\text{-O-Fe}^{3+}$.

The knowledge of field dependence of magnetic entropy change ΔS_M of a magnetic refrigerant material is important [35]. Understanding the field dependence can provide further clues to improve the performance of refrigerant materials in a lower field rather than those needed in already existing prototypes (generally 1–2 T). The field's dependence of the magnetic entropy change curve helps us to predict the response of a particular material under different extreme conditions, which can be useful for designing new materials for magnetic refrigeration [6]. Therefore, a study of the MCE for a particular material is not only important from a practical application point of view but also it provides a tool to understand the properties of the material. In particular, the details of the magnetic phase transition and critical behaviour can be obtained by studying the MCE of the material [36,37].

In this paper, the magnetocaloric properties and the critical behaviour for the optimized $\text{La}_{0.67}\text{Ca}_{0.33}\text{Mn}_{0.9}\text{Fe}_{0.1}\text{O}_3$ compound at several magnetic fields was investigated. The polycrystalline sample was prepared by a solid-state reaction method [34].

2. Model calculations

According to the phenomenological model [38], the dependence of magnetization on variation of temperature and Curie temperature T_C is presented by

$$M(T, H = H_{\max}) = \left(\frac{M_i - M_f}{2} \right) [\tanh(A(T_C - T))] + BT + C, \quad (1)$$

where H_{\max} is the maximum external field, T_C the Curie temperature; M_i/M_f the initial/final value of magnetization at ferromagnetic–paramagnetic transition as shown in figure 1. Here,

$$A = 2 \left(\frac{B - S_c}{M_i - M_f} \right),$$

B the magnetization sensitivity dM/dT at ferromagnetic state before transition, S_c the magnetization sensitivity dM/dT at Curie temperature T_C , and $C = ((M_i - M_f)/2) - BT_C$.

The magnetic entropy change (ΔS_M) can be obtained through the adiabatic change of temperature by the application of a magnetic field. ΔS_M as a function of temperature for a field variation from 0 to H_{\max} is given by

$$\Delta S_M(T, \Delta H = H_{\max}) = H_{\max} \left[-A \left(\frac{M_i - M_f}{2} \right) \text{sech}^2(A(T_C - T)) + B \right]. \quad (2)$$

A more abrupt variation of magnetization near the magnetic transition occurs and results in a large magnetic entropy change. ΔS_M depends on the temperature gradient of the magnetization and reaches a maximum value around T_C .

Relative cooling power (RCP) is a useful parameter which decides the efficiency of magnetocaloric materials based on the magnetic entropy change [1,39]. The RCP is defined as the product of the maximum magnetic entropy change $\Delta S_{M\max}$ and full-width at half-maximum in $\Delta S_M(T)$ curve (δT_{FWHM}). According to this model, $\Delta S_{M\max}$ is available by

$$\Delta S_{M\max} = H_{\max} \left[-A \left(\frac{M_i - M_f}{2} \right) + B \right] \quad (3)$$

and δT_{FWHM} is presented by

$$\delta T_{\text{FWHM}} = \frac{2}{A} \cosh^{-1} \left(\frac{2A(M_i - M_f)}{A(M_i - M_f) + 2B} \right)^{1/2}. \quad (4)$$

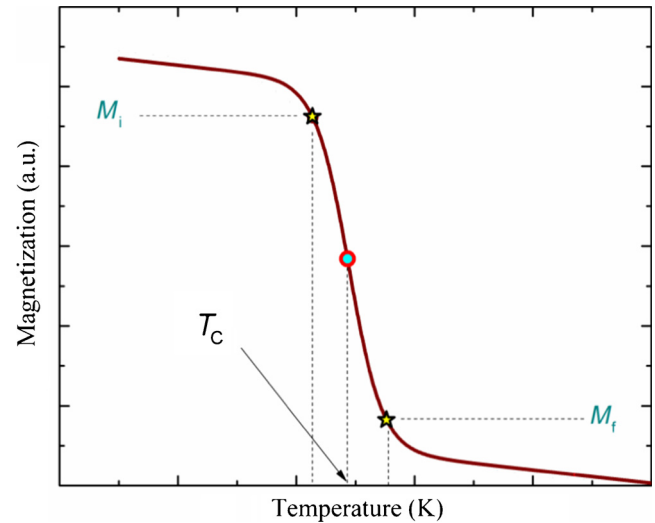


Figure 1. Temperature dependence of magnetization in constant applied magnetic field.

Table 1. Model parameters for $\text{La}_{0.67}\text{Ca}_{0.33}\text{Mn}_{0.9}\text{Fe}_{0.1}\text{O}_3$ at several magnetic fields.

$\mu_0 H$ (T)	M_i (emu g^{-1})	M_f (emu g^{-1})	T_C (K)	B (emu $\text{g}^{-1} \text{K}^{-1}$)	S_C (emu $\text{g}^{-1} \text{K}^{-1}$)
0.05	16.97393	0.45549	105.043	-0.00289	-0.41592
0.1	25.47044	0.56936	106.19	-0.00541	-0.51
0.2	33.14763	0.56936	105.665	-0.00401	-0.49491
0.5	38.14338	2.22846	106.912	-0.00842	-0.49508
1	41.25447	5.65958	109.444	-0.0261	-0.45866
1.5	42.33495	9.47224	110.67	-0.0475	-0.43608
2	45.28089	9.01723	112.563	-0.04024	-0.41307
3	46.31226	14.34203	113	-0.06545	-0.39333

Then RCP is computed by

$$\text{RCP} = -\Delta S_{M,\max} \delta T_{\text{FWHM}} = H_{\max} \left(M_i - M_f - \frac{2B}{A} \right) \times \cosh^{-1} \left(\frac{2A (M_i - M_f)}{A (M_i - M_f) + 2B} \right)^{1/2}. \quad (5)$$

The RCP corresponds to the amount of heat that can be transferred between the cold and hot parts of the refrigerator in one ideal thermodynamic cycle. This parameter allows an easy comparison of different magnetic materials for applications in magnetic refrigeration; hence, larger RCP values lead to better magnetocaloric materials.

Another figure of merit which is used to compare the magnetic refrigerant materials is the refrigerant capacity (RC). The RC can be determined by numerically integrating the area under the $\Delta S_M(T)$ curve using the temperatures at half-maximum of the peak as the integration limits [40]. Here, RC value can be obtained as

$$\begin{aligned} \text{RC} &= - \int_{T_C - \frac{\delta T_{\text{FWHM}}}{2}}^{T_C + \frac{\delta T_{\text{FWHM}}}{2}} \Delta S(T) dT \\ &= H_{\max} \left[- (M_i - M_f) \tanh \left(A \frac{\delta T_{\text{FWHM}}}{2} \right) + B \delta T_{\text{FWHM}} \right]. \end{aligned} \quad (6)$$

The heat capacity can be calculated from the magnetic contribution to the entropy change induced in the material, $\Delta C_{P,H}$, by the following expression:

$$\Delta C_{P,H} = T \frac{\partial \Delta S_M}{\partial T}. \quad (7)$$

From this model, a determination of $\Delta C_{P,H}$ can be carried out as follows:

$$\begin{aligned} \Delta C_{P,H}(T, \Delta H = H_{\max}) &= H_{\max} \left[-T A^2 (M_i - M_f) \text{sech}^2(A(T_C - T)) \times \tanh(A(T_C - T)) \right]. \end{aligned} \quad (8)$$

From this phenomenological model, it can easily assess the values of ΔT_{FWHM} , $\Delta S_{M,\max}$, RCP RC and $\Delta C_{P,H \min/\max}$ for $\text{La}_{0.67}\text{Ca}_{0.33}\text{Mn}_{0.9}\text{Fe}_{0.1}\text{O}_3$ at several magnetic fields.

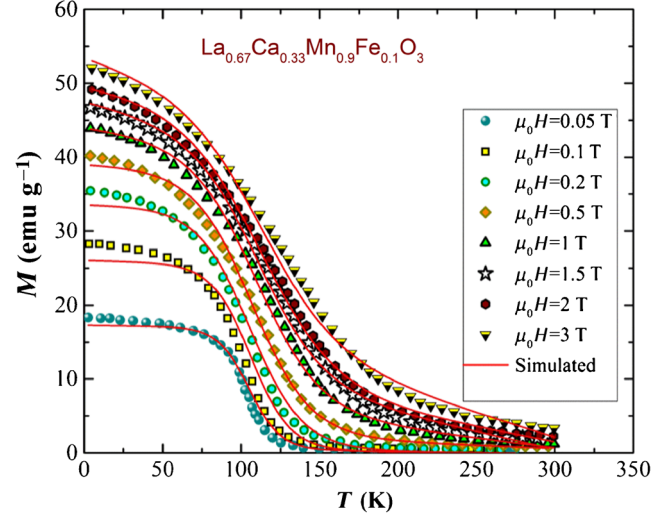


Figure 2. Magnetization vs. temperature for the $\text{La}_{0.67}\text{Ca}_{0.33}\text{Mn}_{0.9}\text{Fe}_{0.1}\text{O}_3$ system at several magnetic fields. The solid lines are modelled results and symbols represent experimental data from reference [34].

3. Model application and discussions

In order to predict the thermomagnetic properties for $\text{La}_{0.67}\text{Ca}_{0.33}\text{Mn}_{0.9}\text{Fe}_{0.1}\text{O}_3$, numerical calculations were made with parameters as displayed in table 1. Figure 2 depicts the magnetization vs. temperature in different applied magnetic field shifts for $\text{La}_{0.67}\text{Ca}_{0.33}\text{Mn}_{0.9}\text{Fe}_{0.1}\text{O}_3$ prepared by the solid-state reaction method as described elsewhere [34]. The symbols represent experimental data from reference [34], while the solid curves represent modelled data using model parameters given in table 1. It is seen that for the given parameters, the results of calculation are in good accordance with the experimental results. The substitution of the manganese with the iron in the parent compound $\text{La}_{0.67}\text{Ca}_{0.33}\text{MnO}_3$ leads to introduce the quenched disorder and has modified the nature of the phase transition from the first-order to the second-order-like [34]. Consequently magnetic transition in $\text{La}_{0.67}\text{Ca}_{0.33}\text{Mn}_{0.9}\text{Fe}_{0.1}\text{O}_3$ is reversible in a cycle of increasing and decreasing temperature and the thermal hysteresis losses have been reduced which is highly desired in the sense of practical application. It can be

reported that the magnetization exhibits a continuous change around T_C in different magnetic fields [34].

Furthermore, figures 3 and 4 show predicted values for changes of magnetic entropy and specific heat. Magnetic entropy change in $\text{La}_{0.67}\text{Ca}_{0.33}\text{Mn}_{0.9}\text{Fe}_{0.1}\text{O}_3$ is reported for $\mu_0 H = 0.05, 0.1, 0.2, 0.5, 1, 1.5, 2$ and 3 T in figure 3 and shows an increase in $-\Delta S_M$ with increasing $\mu_0 H$. The $-\Delta S_M$ is found to be positive in the entire temperature range for all magnetic fields confirmed the ferromagnetic character. It is seen that the results of calculation are in a good agreement with the experimental results. The MCE increases with the increase of the applied magnetic field and with the change of magnetization during application of magnetic field. This means that the effect reaches its maximum in the vicinity of magnetic phase transition points. The large values of $-\Delta S_M$ for $\text{La}_{0.67}\text{Ca}_{0.33}\text{Mn}_{0.9}\text{Fe}_{0.1}\text{O}_3$ compounds originate from a reversible second-order magnetic transition [34]. The magnetic transition becomes broader and so gives rise to a larger broadening of the $-\Delta S_M$ [41]. The broad magnetic entropy peaks are advantage for magnetic cooling system [42].

Using equation (8) one can calculate the specific heat changes, $\Delta C_{P,H}$ caused by the applied magnetic field. Shown in figure 4 is $\Delta C_{P,H}$ as a function of temperature for $\mu_0 H = 0.05, 0.1, 0.2, 0.5, 1, 1.5, 2$ and 3 T. It is clearly seen that $\Delta C_{P,H}$ changes sharply from the negative to the positive at the Curie temperature. Since $\partial M/\partial T < 0$; $\Delta S_M < 0$ results, and accordingly the total entropy decreases upon magnetization. Furthermore, $\Delta C_{P,H} < 0$ for $T < T_C$ and $\Delta C_{P,H} > 0$ for $T > T_C$ [43,44]. The sum of the two parts is the magnetic contribution to the total specific heat which affects the cooling or heating power of the magnetic refrigerator [45]. Specific heat presents the advantage of delivering values necessary for further refrigerator design, should the material in question be selected.

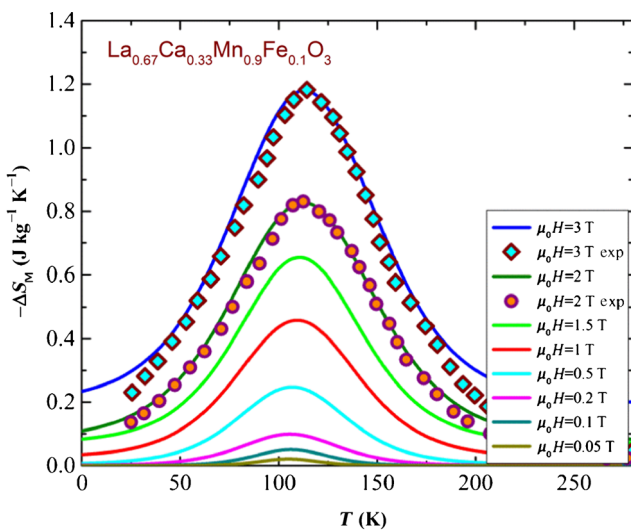


Figure 3. Magnetic entropy change, ΔS_M , for the $\text{La}_{0.67}\text{Ca}_{0.33}\text{Mn}_{0.9}\text{Fe}_{0.1}\text{O}_3$ sample. The solid lines are predicted results and symbols represent experimental data from reference [34].

The MCE data of different materials of same universality class should fall onto the same curve irrespective of the applied magnetic field [46]. Because of the intrinsic relation between the MCE and the universality class, one can obtain the critical exponents based on the MCE data, which may be another method for determining the critical behaviour of phase transition, i.e., the universality class. Using the magnetocaloric response (or magnetic entropy change), one can investigate the nature of these coupled order parameters and further understand the rich magnetic properties exhibited by $\text{La}_{0.67}\text{Ca}_{0.33}\text{Mn}_{0.9}\text{Fe}_{0.1}\text{O}_3$ manganites. At the peak, the field dependence of $-\Delta S_M$ can be assumed to be a power law, with an exponent n

$$\Delta S_{\max} \approx a (\mu_0 H)^n. \quad (9)$$

At T_C , the exponent n becomes field independent and is expressed as

$$n(T_C) = \left(\frac{\beta - 1}{\beta + \gamma} \right) + 1, \quad (10)$$

where β and γ are the critical exponents [7,47]. With the Widom relation $\delta = 1 + \gamma/\beta$ [48], relation (10) can be written as

$$n(T_C) = \frac{1}{\delta} \left(1 - \frac{1}{\beta} \right) + 1. \quad (11)$$

As shown in figure 5 the fitting of full square points (ΔS_{\max}) leads to that $n(T_C) = 0.710(2)$ for $\text{La}_{0.67}\text{Ca}_{0.33}\text{Mn}_{0.9}\text{Fe}_{0.1}\text{O}_3$, which is larger than the predicted value of $2/3$ in the mean field approach [49] due to the local inhomogeneities in $\text{La}_{0.67}\text{Ca}_{0.33}\text{Mn}_{0.9}\text{Fe}_{0.1}\text{O}_3$.

As discussed above, the width of ΔS_M becomes more and more broad with the increase of field. In order to confirm this result; the field dependence of the full-width at half-maximum ΔT_{FWHM} is given in figure 5. It is found that

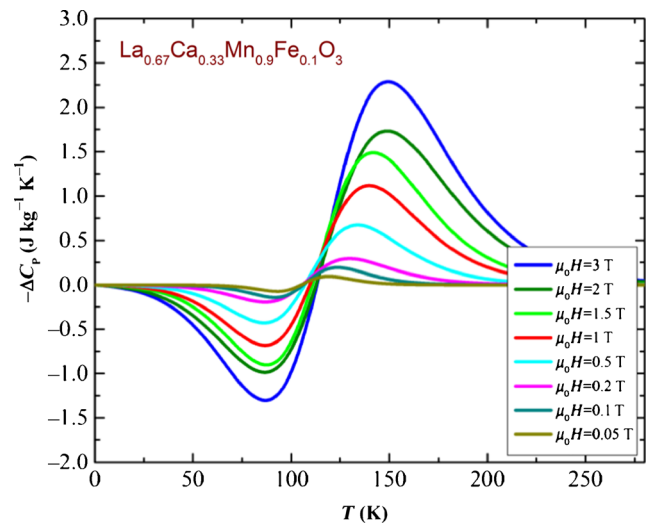


Figure 4. Heat capacity change, ΔC_p , for $\text{La}_{0.67}\text{Ca}_{0.33}\text{Mn}_{0.9}\text{Fe}_{0.1}\text{O}_3$ system at several magnetic fields.

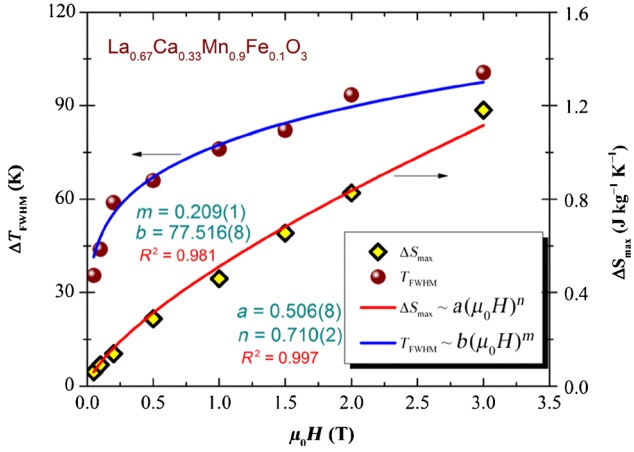


Figure 5. Field dependence of ΔS_{max} and ΔT_{FWHM} for $\text{La}_{0.67}\text{Ca}_{0.33}\text{Mn}_{0.9}\text{Fe}_{0.1}\text{O}_3$.

ΔT_{FWHM} is also field dependent. The fitness of ΔT_{FWHM} gives that $\Delta T_{\text{FWHM}} \approx b(\mu_0 H)^m$ where $b = 77.516(8)$ and $m = 0.209(1)$.

In addition to the magnitude of the ΔS_{M} , other important parameters used to characterize the refrigerant efficiency of the material are the RCP and the RC defined as equations (5) and (6). RCP and RC give an estimate of quantity of the heat transfer between the hot (T_{hot}) and cold (T_{cold}) end during one refrigeration cycle and is the area under the ΔS_{M} vs. T curve between two temperatures ($\Delta T = T_{\text{hot}} - T_{\text{cold}}$) of the full-width at half-maximum (FWHM) of the curve. Figure 6 shows the values for the compound $\text{La}_{0.67}\text{Ca}_{0.33}\text{Mn}_{0.9}\text{Fe}_{0.1}\text{O}_3$ as a function of applied magnetic field.

To analyse the nature of the magnetic phase transition in detail, a critical exponent's study near their Curie temperature (T_{C}) for the $\text{La}_{0.67}\text{Ca}_{0.33}\text{Mn}_{0.9}\text{Fe}_{0.1}\text{O}_3$ sample was carried out. In this context, the field dependence of ΔS_{M} is used for investigating the critical behaviour [50,51]. On the basis of figure 6, the field dependence of the RCP for $\text{La}_{0.67}\text{Ca}_{0.33}\text{Mn}_{0.9}\text{Fe}_{0.1}\text{O}_3$ is depicted. It can be expressed as a power law by taking account of the field dependence of entropy change ΔS_{M} and reference temperature into consideration $\text{RCP} = v(\mu_0 H)^w$ (where $w = 1 + 1/\delta$, v is a constant and δ the critical exponent of the magnetic transition), as predicted by scaling laws [35]. This feature provides insight into the critical behaviour of the compound. The lowest field data have been omitted because of the large uncertainty of the peak position. The slope of the linear function fitted to the Ln–Ln data yields the value of $w \approx 1.208(7)$ which implies $\delta = 4.791(5)$.

The knowledge of two critical exponents n and δ inferred from the field dependence of MCE is enough to determine other exponents, β and γ . By means of the Widom relation, equations (10) and (11) one effortlessly finds $\beta = 1/(\delta(1 - n) + 1) \approx 0.418(6)$, and $\gamma = \beta(\delta - 1) \approx 1.587(3)$. Fundamentally β and γ keep close to the value expected for the 3D Heisenberg ferromagnets with ferromagnetic short-range interactions. A similar result of critical behaviours was

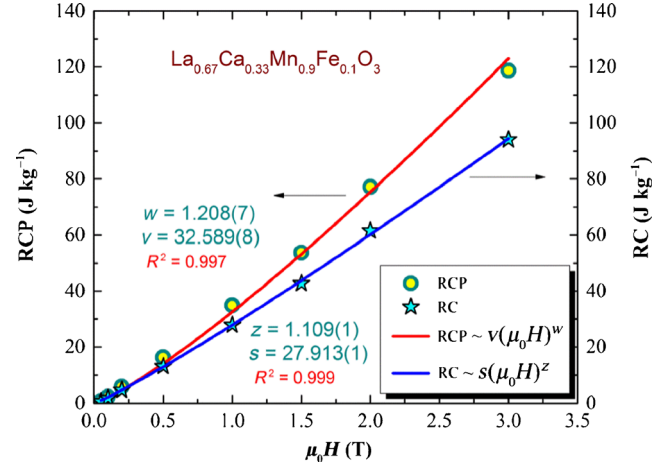


Figure 6. Field dependence of RCP and RC for $\text{La}_{0.67}\text{Ca}_{0.33}\text{Mn}_{0.9}\text{Fe}_{0.1}\text{O}_3$.

observed in Fe-doped LaMnO_3 [52] and ErTiO_3 [46]. The obtained critical exponents of $\text{La}_{0.67}\text{Ca}_{0.33}\text{Mn}_{0.9}\text{Fe}_{0.1}\text{O}_3$, as well as those of different theoretical models, are listed in table 2 for comparison.

Hence, the present study deals with critical and magnetocaloric properties of $\text{La}_{0.67}\text{Ca}_{0.33}\text{Mn}_{0.9}\text{Fe}_{0.1}\text{O}_3$. A precise estimate of the critical exponents for this material near ferromagnetic (FM)–paramagnetic (PM) phase transition temperature is presented and shows that the critical exponents are 3D short-range Heisenberg like in this particular compound. This reflects the existence of FM short-range order in $\text{La}_{0.67}\text{Ca}_{0.33}\text{Mn}_{0.9}\text{Fe}_{0.1}\text{O}_3$. The mixed valence of Mn and Fe ions promotes both the FM double-exchange and AFM super-exchange interactions and thus leads to inhomogeneous regions in magnetism.

In recent times, the authors [22,26,53] and others [54,55] have shown that for second-order magnetic transition materials the $\Delta S_{\text{M}}(T)$ curves obtained with different maximum applied fields will collapse onto a universal curve by normalizing all the ΔS_{M} curves with their peak entropy change, respectively, as $\Delta S_{\text{M}}' = \Delta S_{\text{M}}/2$, and the temperature axis has to be rescaled in a different way below and above T_{C} , just by imposing that the position of two additional reference points in the curve correspond to new parameter θ , defined by the expression [26,56]

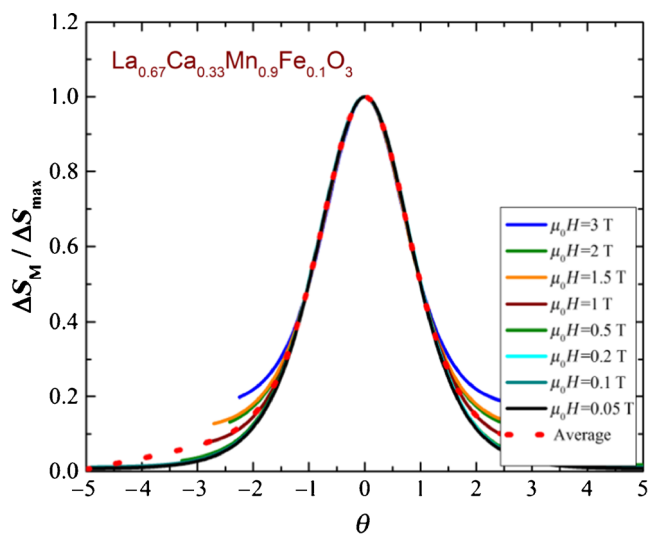
$$\theta = \begin{cases} -(T - T_{\text{C}}) / (T_{\text{r1}} - T_{\text{C}}); & T \leq T_{\text{C}}, \\ (T - T_{\text{C}}) / (T_{\text{r2}} - T_{\text{C}}); & T > T_{\text{C}}, \end{cases} \quad (12)$$

where T_{r1} and T_{r2} are the reference temperatures below and above T_{C} , respectively.

The phenomenological construction of the universal scaling of different magnetic field is depicted in figure 7. Figure 7 shows an attempt to form a master curve for the entropy change of the $\text{La}_{0.67}\text{Ca}_{0.33}\text{Mn}_{0.9}\text{Fe}_{0.1}\text{O}_3$. One can see that the universal behaviour manifests itself only in a limited interval around the peak temperature. Farther below and above the peak the scaling behaviour apparently breaks. Increasing fields produce an increase in the reduced magnetic

Table 2. Critical exponents of materials obtained from the MCE scaling law method and theoretical values of three models.

Composition	n	β	γ	δ	Ref.
La _{0.67} Ca _{0.33} Mn _{0.9} Fe _{0.1} O ₃	0.710(2)	0.418(6)	1.587(3)	4.791(3)	Present
DyTiO ₃	0.621(4)	0.352(2)	1.355(3)	4.85(2)	[46]
HoTiO ₃	0.679(3)	0.397(5)	1.476(4)	4.72(6)	[46]
ErTiO ₃	0.710(7)	0.413(5)	1.611(6)	4.90(5)	[46]
La _{0.6} Pr _{0.4} Fe _{10.7} Co _{0.8} Si _{1.5}	0.773(5)	0.560(5)	1.381(1)	3.463(9)	[36]
Tricritical mean-field model	—	0.25	1.0	5.0	[61]
Mean-field model	—	0.5	1.0	3.0	[61]
3D Heisenberg model	—	0.365	1.386	4.8	[61]
3D Ising model	—	0.325	1.24	4.82	[61]

**Figure 7.** Normalized entropy change as a function of the rescaled temperature θ (the dash curve is averaged).

entropy change. Deviations from the collapse might indicate either the influence of the demagnetizing field associated to the shape of the sample [57] or the presence of additional magnetic phases [58,59]. The divergence of the curves is clear in the compound, particularly above the T_C . As you can see, this universal curve is independent of the external measurement conditions, which is just determined by the intrinsic magnetization.

On the basis of the universal scaling, an average curve is obtained, as shown as dashed curve in figure 7 which gives a smoother description of the curve. This average curve, once the temperature axis is back transformed from the reduced temperature to the unnormalized one, allows making extrapolations to lower temperatures for the high field data and obtaining a finer description of the peak for the low field curves [60].

4. Conclusions

In summary, the exhibition of large MCE in La_{0.67}Ca_{0.33}Mn_{0.9}Fe_{0.1}O₃ which is associated with a FM to PM phase transition near the Curie temperature was reported.

Dependence of the magnetization on temperature variation for La_{0.67}Ca_{0.33}Mn_{0.9}Fe_{0.1}O₃ upon different magnetic fields was simulated. A good RCP value was observed. The large change of magnetization during the phase transition leads to large MCE. It was shown that the higher field La_{0.67}Ca_{0.33}Mn_{0.9}Fe_{0.1}O₃ MCE has a power law field dependence characterized by an exponent $n = 0.710(2)$. The critical exponents associated with FM transition have been determined from the MCE methods. Therefore, the MCE scaling laws can be applied to complex magnetic systems involving different magnetization processes in the critical region. Furthermore, the ΔS_M collapse onto a universal curve based on the scaling relation, where an average curve was obtained. This sample exhibits considerably no magnetic hysteresis, which was beneficial for the magnetic cooling efficiency. In this respect, the lanthanum manganites based materials are very promising refrigerants because of (1) high safety, (2) easily tuned Curie temperature, (3) relatively low cost of components and fabrication, and (4) being non-toxic.

Acknowledgement

This study was supported by the Tunisian Ministry of Higher Education and Scientific Research.

References

- [1] Tishin A M and Spichkin Y I 2003 *The Magnetocaloric Effect and Its Applications* (Bristol: Institute of Physics Publishing)
- [2] Pecharsky V K and Gschneidner K A Jr 1997 *Phys. Rev. Lett.* **78** 4494
- [3] Pecharsky V K and Gschneidner K A Jr 2001 *Adv. Mater.* **13** 683
- [4] M'nassri R and Cheikhrouhou A 2014 *J. Supercond. Nov. Magn.* **27** 1059
- [5] Mbarek H, M'nassri R, Cheikhrouhou-Koubaa W and Cheikhrouhou A 2014 *Status Solidi A* **211** 975
- [6] Fähler S, Rössler U K, Kastner O, Eckert J, Eggeler G, Emmerich H, Entel P, Müller S, Quandt E and Albe K 2012 *Adv. Eng. Mater.* **14** 10
- [7] De Oliveira N A and Von Ranke P J 2010 *Phys. Rep.* **489** 89
- [8] Phan M H and Yu S C 2007 *J. Magn. Magn. Mater.* **308** 325

- [9] M'nassri R, Chniba Boudjada N and Cheikhrouhou A 2015 *J. Alloys Compd.* **626** 20
- [10] M'nassri R, Cheikhrouhou-Koubaa W, Chniba-Boudjada N and Cheikhrouhou A 2013 *J. Appl. Phys.* **113** 073905
- [11] Choura Maatar S, M'nassri R, Cheikhrouhou Koubaa W, Koubaa M and Cheikhrouhou A 2015 *J. Solid State Chem.* **225** 83
- [12] M'nassri R, Chniba Boudjada N and Cheikhrouhou A 2015 *J. Alloys Compd.* **640** 183
- [13] M'nassri R and Cheikhrouhou A 2014 *J. Supercond. Nov. Magn.* **27** 421
- [14] Akther Hossain A K M, Cohen L F, Kodenkandeth T, Mac Manus-Driscoll J and Mc Nalford N 1999 *J. Magn. Mater.* **195** 31
- [15] Selmi A, Bettaibi A, Rahmouni H, M'nassri R, Chniba Boudjada N, Cheikhrouhou A and Khirouni K 2015 *J. Ceram. Int.* **41** 11221
- [16] M'nassri R and Cheikhrouhou A 2014 *J. Supercond. Nov. Magn.* **27** 1463
- [17] Zener C 1951 *Phys. Rev.* **82** 403
- [18] Millis A J, Littlewood P B and Shraiman B I 1995 *Phys. Rev. Lett.* **74** 5144
- [19] Goodenough J B, Wold A, Arnott R J and Menyuk N 1961 *Phys. Rev.* **124** 373
- [20] M'nassri R, Cheikhrouhou-Koubaa W, Boudjada N and Cheikhrouhou A 2013 *J. Supercond. Nov. Magn.* **26** 1429
- [21] M'nassri R, Cheikhrouhou-Koubaa W, Koubaa M, Boudjada N and Cheikhrouhou A 2011 *Solid State Comm.* **151** 1579
- [22] M'nassri R, Cheikhrouhou-Koubaa W, Kouba M and Cheikhrouhou A 2012 *IOP Conf. Ser: Mater. Sci. Eng.* **28** 012050
- [23] Klein J, Höfener C, Uhlenbruck S, Alff L, Büchner B and Gross R 1999 *Europhys. Lett.* **47** 371
- [24] M'nassri R, Chniba Boudjada N and Cheikhrouhou A 2015 *J. Alloys Compd.* **626** 20
- [25] Lampen P, Puri A, Phan M-H and Srikanth H 2012 *J. Alloys Compd.* **512** 94
- [26] M'nassri R and Cheikhrouhou A 2014 *J. Supercond. Nov. Magn.* **27** 1463
- [27] Phan M H and Yu S C 2007 *J. Magn. Mater.* **308** 325
- [28] Osthöver C, Grünberg P and Arons R R 1998 *J. Magn. Mater.* **854** 177
- [29] Selmi A, M'nassri R, Cheikhrouhou-Koubaa W, Chniba Boudjada N and Cheikhrouhou A 2015 *J. Alloys Compd.* **619** 627
- [30] Barahona P, Pena O, Antunes A B, Campos C, Pecchi G, Moreno Y, Moure C and Gil V 2008 *J. Magn. Mater.* **320** e61
- [31] Selmi A, M'nassri R, Cheikhrouhou-Koubaa W, Chniba Boudjada N and Cheikhrouhou A 2015 *J. Ceram. Int.* **41** 7723
- [32] Mahjoub S, Baazaoui M, M'nassri R, Rahmouni H, Chniba Boudjada N and Oumezzine M 2014 *J. Alloys Compd.* **608** 191
- [33] Chang Y L, Huang Q and Ong C K 2002 *J. Appl. Phys.* **91** 789
- [34] Mukadam M D and Yusuf S M 2009 *J. Appl. Phys.* **105** 063910
- [35] Oumezzine M, Pea O, Kallel S and Oumezzine M 2012 *J. Alloys Compd.* **539** 116
- [36] M'nassri R 2014 *J. Supercond. Nov. Magn.* **27** 1787
- [37] Halder M, Yusuf S M, Mukadam M D and Shashikala K 2010 *Phys. Rev. B* **81** 174402
- [38] Hamad M A 2012 *Phase Transitions* **85** 106
- [39] Gschneidner K A and Pecharsky V K Jr 2000 *Annu. Rev. Mater. Sci.* **30** 387
- [40] Gschneidner K A, Pecharsky V K, Pecharsky A O and Zimm C B 1999 *Mater. Sci. Forum* **315** 69
- [41] El-Hagary M 2010 *J. Alloys Compd.* **502** 376
- [42] Wang A, Liu Y, Zhang Z, Long Y and Cao G 2004 *Solid State Commun.* **130** 293
- [43] Foldeaki M, Chahine R and Bose T K 1995 *J. Appl. Phys.* **77** 3528
- [44] Yang H, Zhu Y H, Xian T and Jiang J L 2013 *J. Alloys Compd.* **555** 150
- [45] Zhang X X, Wen G H, Wang F W, Wang W H, Yu C H et al 2000 *Appl. Phys. Lett.* **77** 3072
- [46] Su Y, Sui Y, Cheng J-G, Zhou J-S, Wang X, Wang Y and Goodenough J B 2013 *Phys. Rev. B* **87** 195102
- [47] Franco V and Conde A 2010 *Int. J. Refrig.* **33** 465
- [48] Stanley H E 1971 *Introduction to Phase Transitions and Critical Phenomena* (London: Oxford University Press)
- [49] Franco V, Blazquez J S and Conde A 2006 *Appl. Phys. Lett.* **89** 222512
- [50] Franco V, Conde A, Romero-Enrique J M and Blazquez J S 2008 *J. Phys. Condens. Matter* **20** 285207
- [51] Zhang X X, Tejada J, Xin Y, Sun G F, Wong K W and Bohigas X 1996 *Appl. Phys. Lett.* **69** 3596
- [52] Phan T-L, Thanh P Q, Yen P D H, Zhang P, Thanh T D and Yu S C 2013 *Solid State Commun.* **167** 49
- [53] M'nassri R and Cheikhrouhou A 2014 *J. Korean Phys. Soc.* **64** 879
- [54] Franco V, Conde A, Pecharsky V K and Gschneidner K A Jr 2007 *Europhys. Lett.* **79** 47009
- [55] Franco V, Conde A, Sidhaye D, Prasad B L V, Poddar P, Srinath S, Phan M H and Srikanth H 2010 *J. Appl. Phys.* **107** 09A902
- [56] Franco V, Blazquez J S and Conde A 2006 *Appl. Phys. Lett.* **89** 222512
- [57] Caballero-Flores R, Franco V, Conde A and Kiss L F 2009 *J. Appl. Phys.* **105** 07A919
- [58] Franco V, Conde A, Provenzano V and Shull R D 2010 *J. Magn. Mater.* **322** 218
- [59] Franco V, Caballero-Flores R, Conde A, Dong Q Y and Zhang H W 2009 *J. Magn. Mater.* **321** 1115
- [60] Zhang L, Fan J, Tong W, Ling L, Pi L and Zhang Y 2012 *Physica B* **407** 3543
- [61] Stanley H E 1999 *Rev. Mod. Phys.* **71** S358